ORGANOMETALLICS

Article

pubs.acs.org/Organometallics

# Macrocyclic Platforms for the Construction of Tetranuclear Oxo and Hydroxo Zinc Clusters

Thomas Cadenbach,[†] James R. Pankhurst,[†] Tommy A. Hofmann,[‡] Massimiliano Curcio,[†] Polly L. Arnold,[†] and Jason B. Love*[,†]

[†]EaStCHEM School of Chemistry, University of Edinburgh, Joseph Black Building, David Brewster Road, Edinburgh EH9 3FJ, U.K.

[‡]Department of Chemistry, Technische Universität München, Lichtenbergstraße 4, D-85747 Garching, Germany

Supporting Information

**ABSTRACT:** The design of ligands that can act as platforms for the controlled, "bottom-up" synthesis of transition-metal clusters is a promising approach to accessing enzymatic mimics and new small-molecule reaction chemistry. This approach is exemplified here through the coordination chemistry of two compartmental Schiff-base calixpyrroles ($H_4L$) that usually act as dinucleating ligands for transition metals. While reactions between $H_4L$ and $Zn\{N(SiMe_3)_2\}_2$ form the expected dinuclear Zn "Pacman" complexes $Zn_2(L)$, reactions with $ZnEt_2$ result in the tetranuclear Zn alkyl complexes $Zn_4Et_4(THF)_4(L)$, in which open, "bowl-shaped" structures are adopted due to the flexibility of the macrocyclic platform. The outcome of hydrolysis reactions of these tetranuclear complexes is found to depend on the macrocyclic cavity size, with the smaller macrocycle favoring oxo formation in $Zn_4(\mu_4\text{-}O)Et_2(L)$ and the larger macrocycle favoring complete hydrolysis to form the hydroxide-bridged cluster $Zn_4(\mu_2\text{-}OH)_4(L)$. This latter complex reacts with carbon dioxide at elevated temperature, re-forming the free macrocycle $H_4L$ and eliminating $ZnCO_3$.

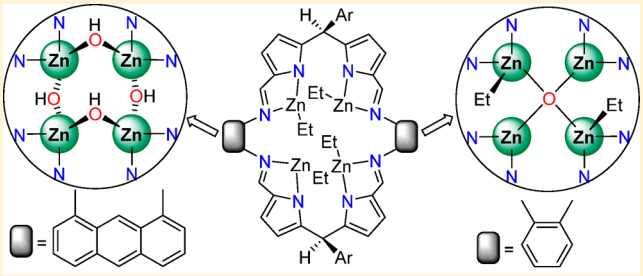


## INTRODUCTION

Clusters and aggregations of transition metals are often found to be the active sites of enzymatic systems that catalyze transformations of small molecules important to sustainable chemical and energy challenges.[1,2] As such, there has been a long-held interest in the development of structural and, in particular, functional models of these evolved biological catalysts, aiming to understand their modes of actions and ultimately generate industrially relevant counterparts.[3−7]

A particularly successful approach to reactive cluster synthesis has been to design multidentate ligands that act as platforms for the "bottom-up" synthesis of complexes of increasingly nuclearity and complexity.[8−15] The Mn−Ca oxo cubane motif found at the oxygen-evolving center in Photosystem II appears common to biological, homogenous, and heterogeneous systems,[6,16] and has been most accurately modeled by building a $Mn_3Ca$ cubane through the capping of a trigonal $Mn_3$ cluster of a polypyridyl-arene trinucleating ligand.[10,17] Trinucleating aminoamide ligands have been used in the preparation and study of low-coordinate, low-crystal-field trigonal $Fe_3$ clusters relevant to the FeMo cofactor of nitrogenases,[18,19] and trinucleating diketimine cyclophanes facilitate the assembly of trinuclear Cu clusters that can activate dinitrogen.[20]

We have developed Schiff-base pyrrole macrocycles similar to those in Scheme 1 as dinucleating ligands for transition metals and the f elements,[21] and have found that the incorporation of aryl spacers between the two $N_4$-donor compartments generally results in "Pacman"-shaped structures on metalation which provide a well-defined dinuclear reaction environment for small-molecule activation.[22−24] Although rare, higher nuclearity, trimetallic complexes of these macrocycles have been made as a consequence of uranyl activation chemistry,[25−27] and aerobic ring-opening reactions in the presence of Zn cations result in [3 + 3] trinucleating macrocycles and their Zn complexes.[28] Furthermore, hydrolysis of the Mg "Pacman" complex $Mg_2(L)$ results in the spontaneous assembly of the macrocycle encapsulated Mg hydroxide cubane $\{Mg(OH)_2\}_4(H_4L)_2$, in which the two protonated macrocycles adopt orthogonal bowl-shaped geometries and stabilize the cubane through coordination and hydrogen bonding.[29] Recently, we developed the new Schiff-base calixpyrroles $H_4L^{a/b}$, in which the meso carbons are only singly substituted (Scheme 1) to favor oxidation to dipyrrins.[30] While we were unsuccessful in this regard, the decreased steric hindrance at the meso carbon resulted in greater structural adaptability in comparison to that in previous macrocycle generations, with Cu complexes adopting unusual bowl-shaped instead of Pacman-shaped structures. As such, we anticipated that these more structurally versatile macrocyclic ligands might favor cluster synthesis and herein we report their

**Special Issue:** Mike Lappert Memorial Issue

**Received:** December 5, 2014




DOI: 10.1021/om501244n
*Organometallics* XXXX, XXX, XXX−XXX

**Scheme 1. Synthesis of Di- and Tetranuclear Zn Complexes of the Schiff-Base Calixpyrroles $H_4L^{a/b}$ (N′′ = $N(SiMe_3)_2$)**

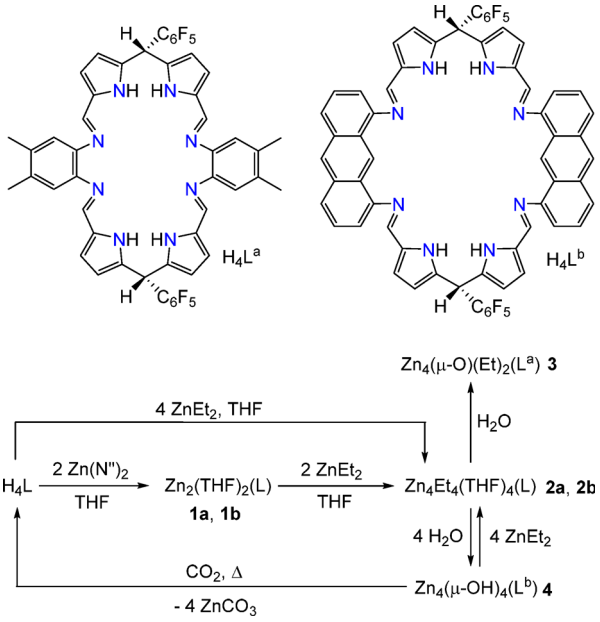


use as platforms for the generation of di- and tetranuclear Zn clusters.

## RESULTS AND DISCUSSION

**Dinuclear Zinc Complexes.** The dinuclear Zn(II) complexes $Zn_2(THF)_2(L)$ (L = $L^a$ (**1a**), $L^b$ (**1b**)) were prepared in high yields (70−90%) from the respective reactions of the macrocycles $H_4L^a$ and $H_4L^b$ with 2 equiv of $Zn\{N(SiMe_3)_2\}_2$ (Scheme 1).

The $^1$H NMR spectrum for **1a** indicates a symmetric product with a single set of resonances for the macrocycle. Deprotonation of the pyrrole nitrogens is indicated by the presence of free $HN(SiMe_3)_2$ at 0.10 ppm and the disappearance of the N−H resonance of the macrocycle, and the meso proton has shifted to 6.99 ppm from 5.88 ppm in $H_4L^a$. The MALDI-TOF mass spectrum of **1a** (see the Supporting Information) shows a molecular ion at $m/z$ 1063 with an isotope distribution consistent with a dinuclear zinc complex.

The $^1$H NMR spectrum for **1b** indicates that two symmetric products are formed from the reaction in a 3/1 ratio, which suggests the presence of two macrocyclic isomers in solution, presumably with Pacman structures in which the meso protons are endo or exo to the macrocyclic cleft. Crystals of **1b** were grown from a THF solution and the solid-state structure determined by X-ray crystallography (Figure 1).

In the solid state, the macrocycle adopts a Pacman configuration and coordinates one Zn(II) center in each $N_4$-donor pocket. One THF solvent molecule is coordinated to each Zn atom on the exo face, resulting in a distorted-square-pyramidal coordination geometry for each Zn (sum of $N_4$-equatorial bond angles 352.2°) and an internuclear separation of 6.236(1) Å. Importantly, **1b** crystallizes as the syn-endo isomer, with the $C_6F_5$ groups pointing into the macrocycle cleft. Previously, only the syn-exo isomer has been observed for $H_4L^b$ and its copper complex, both in solution and in the solid state.[30]

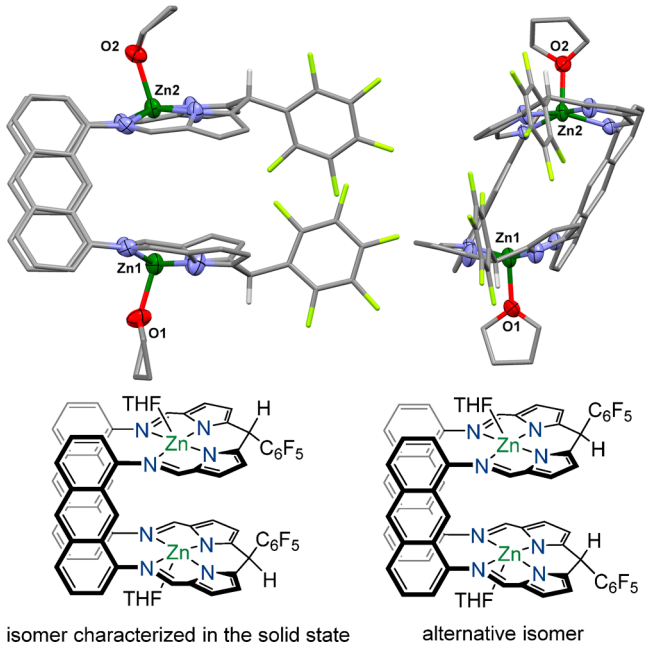


**Figure 1.** (top) Solid-state structure of $Zn_2(THF)_2(L^b)$ (**1b**). For clarity, the solvent of crystallization and all hydrogen atoms, except those on the *meso*-C, are omitted (where shown, displacement ellipsoids are drawn at 50% probability). ChemDraw representations of both of the possible isomers seen in solution are also shown (bottom).

We, and others, have characterized Zn complexes of macrocycles similar to $L^{a/b}$ that are doubly substituted at the meso carbon. The zinc chemistry of $H_4L^{a\text{-}R2}$ (i.e., two alkyl meso substituents, *o*-phenylene spacer) is not straightforward, resulting in the isolation of expanded macrocyclic complexes (see above)[28] or fluoride-bridged complexes resulting from F-abstraction chemistry, e.g. $[Zn_2(\mu\text{-}F)_2(H_4L^{a\text{-}R2})][BF_4]_2$;[31] in all of these complexes the pyrrole nitrogens remain protonated. For $H_4L^{b\text{-}R2}$ (anthracenyl spacer), the Zn chemistry is similar to that seen for $L^b$, although the simple $Zn_2(L^{b\text{-}R2})$ complexes were found to be complex aggregates in solution and only form crystalline materials in the presence of anions such as $Cl^-$ and $OH^-$, which were accommodated within the dinuclear macrocyclic cleft.[32] In these latter compounds, Zn···Zn separations determined by X-ray crystallography ranged from 3.871(1) Å ($\mu$-OH) to 4.532(1) Å ($\mu$-Cl), and the structure of anion-free $Zn_2(L^{b\text{-}R2})$, determined by DFT calculations, displays a Zn···Zn separation of 4.98 Å. The distances are considerably shorter than those in **1b** and reflect the flexibility of the $N_4$-donor set, which facilitates distortion of the Zn cation out of the $N_4$ plane into the cleft; in **1b** this movement is exogenous to the cleft due to binding to THF.

**Tetranuclear Zinc Complexes.** In contrast to reactions involving zinc silylamide, the reactions between $H_4L$ and $ZnEt_2$ do not form the dinuclear complexes **1a,b** but instead form the tetranuclear complexes $Zn_4Et_4(THF)_4(L)$ (**2a,b**) (Scheme 1). The solid-state structure of **2b** was determined by X-ray crystallography and shows that each Zn(II) center is coordinated to a single imino-pyrrole chelate in the macrocycle and each Zn(II) center has retained an ethyl group and a molecule of THF (Figure 2). In order to accommodate four ZnEt(THF) units, the macrocycle adopts a bowl-shaped structure,[21] hinging at the meso carbon with a wide bite-angle of 162.1(1)°; previous complexes of anthracene-bridged


DOI: 10.1021/om501244n
Organometallics XXXX, XXX, XXX−XXX

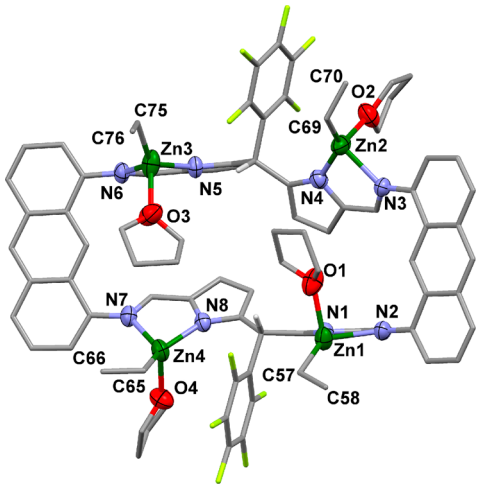


**Figure 2.** Bowl-shaped, solid-state structure of $Zn_4Et_4(THF)_4(L^b)$ (**2b**). For clarity, the solvent of crystallization, minor crystallographic disorder components, and all hydrogen atoms except those on the *meso*-C are omitted (where shown, displacement ellipsoids are drawn at 50% probability).

macrocycles have only been observed to adopt Pacman configurations. High nuclearity, bowl-shaped zinc clusters have also been generated using calixarene platforms.[33] The internuclear separations in **2b** are large due to this bowl configuration, in the range 6.981(3)−7.192(1) Å between nearest neighbors.

The $^1$H NMR spectra for both **2a**,**b** show symmetric compounds with four magnetically equivalent ethyl groups per macrocycle at 1.32 and 0.42 ppm for **2a** ($C_6D_6$) and at 0.99 and 0.12 ppm for **2b** ($d_8$-THF). The $^{19}F\{^1H\}$ NMR spectra for **2a**,**b** feature broad, low-intensity resonances for the *o*-F of the $C_6F_5$ meso substituent; when the temperature is raised to 330 K, these resonances increase in intensity and are less broad

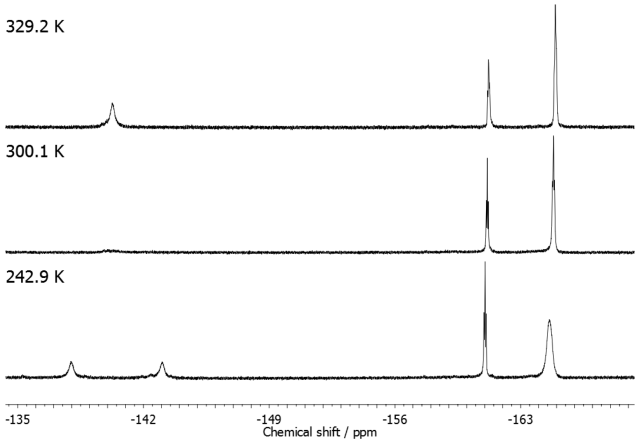


**Figure 3.** Variable-temperature $^{19}F\{^1H\}$ NMR spectra of **2b** in $d_8$-THF.

(Figure 3 and the Supporting Information). In $d_8$-THF, the $^{19}F\{^1H\}$ NMR spectrum for **2a** features broad resonances for both *o*-F and *m*-F positions; on cooling to 243 K, both of these resonances resolve to two resonances each, with the expected multiplicity for their relative environments (see Supporting Information). Such temperature dependence in the $^{19}F\{^1H\}$ NMR spectra was not observed for **1a**,**b** and implies that there is restricted rotation of the $C_6F_5$ group due to the presence of the ZnEt(THF) functionality. However, no nuclear Overhauser interactions were observed between the *o*-F and ethyl groups at 300 or 243 K using $^{19}F-^1H$-HOESY experiments, despite a separation of 2.8−3.0 Å between ethyl groups and *o*-F atoms in the solid state.

While the $^1$H NMR spectrum for **2b** in $d_8$-THF is temperature independent, the spectrum for **2a** features broadened resonances at room temperature that sharpen at 329 K (see Supporting Information). At 243 K, the $^1$H NMR spectrum for **2a** resolves to give two sets of resonances of 1:1 intensity for all resonances with the exception of the meso proton. The temperature and solvent dependence of the $^1$H NMR spectrum for **2a** is best interpreted for **2a** adopting a bowl structure. As the meso protons are located on the hinge of the macrocycle, they are equivalent at low temperature. Torsional flexing of the macrocycle about this hinge produces a $C_2$-symmetric structure that renders each proton environment equivalent at higher temperatures; at low temperature, this symmetry is broken due to the thermal barrier for the flexing mode, and this barrier is raised in the presence of coordinating solvent occupying the cleft.

Conversion of **1a** to **2a** and also of **1b** to **2b** was achieved on addition of 2 equiv of $ZnEt_2$ to the dinuclear complexes, with the *o*-F resonances in both $^{19}F\{^1H\}$ NMR spectra broadened on addition of $ZnEt_2$ and the $^1$H NMR spectra for both products identical with those of **2a**,**b**. Importantly, the resonances for the ethyl groups are equivalent, indicating a conversion to **2a**,**b** by alkyl transfer from one Zn center to another in each pocket. This conversion also reveals a change in the anthracene-bridged macrocycle configuration, from a Pacman structure in **1b** to a bowl structure in **2b**.

**Zinc Oxo and Hydroxo Clusters.** Several attempts were made to determine the solid-state structure of **2a** by X-ray crystallography. However, due to its high sensitivity to trace moisture only the hydrolysis product $Zn_4(\mu_4\text{-O})Et_2(L^a)$ (**3**) was found to crystallize (Figure 4). In the solid-state structure of **3**, the macrocycle adopts a Pacman geometry of $C_{2v}$ symmetry. Two of the Zn(II) centers are bound by pyrrole nitrogen atoms in each pocket, while the other two Zn(II) centers are coordinated by bridging imine-N atoms on each *o*-phenylene group; these imino-Zn centers have retained their

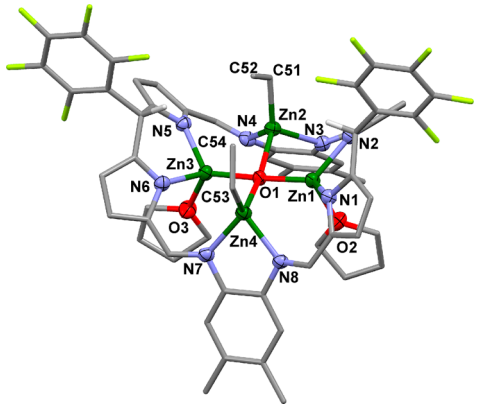


**Figure 4.** Solid-state structure of $Zn_4(\mu_4\text{-O})Et_2(L^a)$ (**3**). For clarity, the solvent of crystallization, minor crystallographic disorder components, and all hydrogen atoms except those on the *meso*-C are omitted (where shown, displacement ellipsoids are drawn at 50% probability).


DOI: 10.1021/om501244n
*Organometallics* XXXX, XXX, XXX−XXX

ethyl groups. A central oxo anion is bound to each Zn center and is best described as acting as an L-type donor to the two pyrrolide-Zn centers and an X-type donor to the two imino-Zn centers, resulting in a charge-neutral complex. The bridging $\mu_4$-oxo anion in the $Zn_4O$ core results in extremely short Zn−Zn distances of 2.8604(6)−2.8371(6) Å, and the core itself is near-planar, with adjacent Zn−O−Zn bond angles of 90° and nonequivalent opposite Zn−O−Zn bond angles of 160.45(12) and 174.81(14)°.

While the $Zn_4(\mu\text{-O})$ structural motif has been characterized numerous times,[34] (187 CSD hits, Zn−O−Zn angle 108.8 ± 6.7°) ,including with associated alkyl groups, e.g. $Zn_4Et_n(\mu\text{-O})$,[35,36] with the exception of Zn hydroxo cubanes, these complexes subtend an almost tetrahedral geometry at the oxygen atom; to our knowledge, the planar environment for oxygen O1 in **3** is unique and is presumably enforced by the more rigid macrocyclic architecture. This, along with the short Zn···Zn separations, led us to carry out DFT calculations on **3** to explore the nature of the bonding between the four zinc centers and the oxygen atom.

The X-ray crystal structure for **3** was accurately represented by the B3LYP functional and 6-31G(d,p) basis set, with less than 1.0% relative error in important bond parameters (see the Supporting Information). Natural bond orbital (NBO) population analysis indicates that the most significant bonding interactions in the $C_{2v}$ $Zn_4O$ cluster arise from $\sigma$ donation from the central oxo anion into unoccupied 4s and 4p orbitals on the four zinc centers. Specifically, there is a $b_1$ set of atomic orbitals that combine to describe the $\sigma\{2p_x(O1)—4s(Zn2,4)\}$ interaction and a $b_2$ set that describes the $\sigma\{2p_y(O1)—4s(Zn1,3)\}$ interaction. An $a_1$ $p_z(\pi)$ interaction extending over the $Zn_4O$ cluster also makes a minor contribution to the bonding. While Zn−O d−p($\pi$) orbital interactions are observed, due to the $3d^{10}$ electron configuration for Zn(II), both the bonding and antibonding molecular orbitals are fully occupied and these interactions do not contribute to the bonding. Importantly, no Zn−Zn covalent bonds were observed by molecular orbital calculations or NBO population analysis; thus, it is likely that the proximity of the Zn centers is due to the presence of the oxo group and the constraints of the macrocylic bonding environment.

Addition of 1 equiv of $H_2O$ to **2a** produces a $^1$H NMR spectrum consistent with the solid-state structure of **3**, with two equivalent ethyl groups per macrocycle with resonances at 1.51 and 0.30 ppm. The sharpness of the *o*-F resonance in the room-temperature $^{19}F\{^1H\}$ NMR spectrum further indicates a loss of ethyl groups from the face of the $N_4$-donor pockets and implies a change in geometry from a bowl configuration (as in **2b**) to a Pacman configuration upon partial hydrolysis. Further hydrolysis results in complete loss of the Zn−Et groups, presumably to form the mixed oxo−hydroxide complex $Zn_4(\mu_4\text{-O})(OH)_2(L^a)$; unfortunately, we have been unable to fully characterize this latter complex.

Due to the increased separation between the $N_4$-coordination compartments in the anthracene-bridged macrocycle, the formation of a $Zn_4O$ cluster is not possible. However, complete hydrolysis of **2b** with 4 equiv of $H_2O$ leads to the clean formation of $\{Zn(\mu_2\text{-OH})\}_4(L^b)$ (**4**) (Scheme 1). The $^1$H NMR spectrum of **4** shows a complete loss of the ethyl ligands and the appearance of two nonequivalent hydroxide resonances at 4.14 and 3.36 ppm that are of equal intensity; these resonances are exchanged in a $D_2O$-shake experiment. The solid-state structure of **4** was determined by X-ray crystallography and shows that the Zn(II) centers are coordinated in a similar manner to **2b**, bound to each imino-pyrrole chelate (Figure 5).

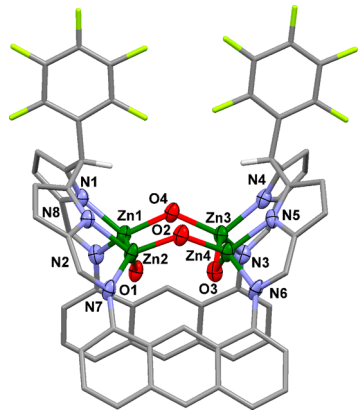


**Figure 5.** Solid-state structure of $\{Zn(\mu_2\text{-OH})\}_4(L^b)$ (**4**). For clarity, the solvent of crystallization and all hydrogen atoms, except those on the *meso*-C, are omitted (where shown, displacement ellipsoids are drawn at 50% probability).

Each Zn(II) center is connected to its two neighbors by a bridging hydroxide, which has the effect of closing the relaxed bowl geometry observed for **2b** to a Pacman geometry of $C_{2v}$ symmetry. The formation of bridging hydroxides also has the effect of shortening the Zn−Zn distances greatly, in the range 3.229(1)−3.4465(9) Å. In order to accommodate this $\{Zn(\mu_2\text{-OH})\}_4$ cluster, the two $N_4$-donor pockets are distorted from their planar arrangement and point into the cleft. The syn-exo isomer of **4** is observed in the solid state and, unlike the case for **1b**, only one isomer is observed in solution, indicating a preferential folding of the bowl structure in **2b**. This simple, molecular $\{Zn(\mu_2\text{-OH})\}_4$ ring structural motif seen in **4** has little precedent. The hexameric complex $\{Zn(\mu\text{-OH})(Bu^t)\}_6$ is formed on hydrolysis of $ZnBu^t_2$ and is an aggregate of two trimeric $\{Zn(\mu\text{-OH})(Bu^t)\}_3$ rings;[37] otherwise, only simple cubanes and extended polymeric structures display a similar formulation and aggregation to **4**.[38]

**Reactions with $CO_2$.** The precedent for insertion and polymerization reactions of carbon dioxide and zinc alkyl or hydroxide complexes[39−41] led us to explore the reactions of **2**−**4** with $CO_2$. Surprisingly, no reactions were seen with **2a**,**b** or **3**, and reaction between $CO_2$ and **4** only occurred at elevated temperature to yield the free macrocycle $H_4L^b$ by $^1$H NMR spectroscopy plus a solid deposit, presumed to be $ZnCO_3$ (Scheme 1). Interestingly, this latter reaction closes a potential cycle for the conversion of $CO_2$ into $ZnCO_3$, albeit not catalytically, and the use of the necessary Zn reagents would make this an undesirably expensive option for $CO_2$ sequestration.[42]

## CONCLUSION

The Schiff-base pyrrole macrocycles $L^{a/b}$ act as platforms for the preparation of Pacman- and bowl-shaped di- and tetranuclear zinc complexes, depending on the nature of the Zn(II) precursor. Significantly, the use of $ZnEt_2$ favors the formation of bowl-shaped tetranuclear organometallic zinc macrocyclic complexes. These complexes undergo controlled hydrolysis, the products of which depend on the arene spacer between the $N_4$-donor compartments. The relative rigidity of


DOI: 10.1021/om501244n
*Organometallics* XXXX, XXX, XXX−XXX

the macrocyclic frameworks means that unusual planar oxo and cyclic hydroxo tetranuclear zinc complexes are formed cleanly, without decomposition to extended aggregates. In a manner similar to our previous work on macrocycle encapsulated magnesium hydroxide cubanes, it is clear that these macrocyclic ligands can flex to accommodate small Zn(OH/O) clusters and limit further cluster growth. We are currently expanding this chemistry to redox-active first-row transition metals.

## EXPERIMENTAL SECTION

**General Procedures.** Syntheses of all compounds were carried out under a $N_2$ atmosphere using standard Schlenk-line techniques. Ligands $H_4L^a$ and $H_4L^b$ were prepared according to literature procedures.[30] Vacuum Atmospheres and MBraun gloveboxes were used to manipulate and store air- and moisture-sensitive compounds under an atmosphere of dried and deoxygenated $N_2$. All gases were supplied by BOC Gases UK. All glassware was dried in an oven at 160 °C, cooled under $10^{-3}$ mbar vacuum, and then purged with $N_2$. Organic solvents were collected from the Vacuum Atmospheres solvent tower drying system, where they had been passed over a column of molecular sieves for 24 h prior to collection; they were then degassed prior to use and subsequent storage over 4 Å molecular sieves. The solvents $d_8$-THF and $C_6D_6$ were dried over K metal, distilled under reduced pressure, and degassed prior to storage under $N_2$. All solvents were supplied by Sigma-Aldrich or Fisher Scientific. NMR spectra were recorded on Bruker AVA400, AVA500, and PRO500 spectrometers. $^1$H and $^{13}C\{^1H\}$ NMR chemical shifts are referenced to residual solvent resonances calibrated against an external standard ($SiMe_4$, $\delta$ 0 ppm). $^{19}F\{^1H\}$ NMR chemical shifts are referenced to an external standard ($CCl_3F$, $\delta$ 0 ppm). X-ray crystallographic data were collected at 170 K on an Oxford Diffraction Excalibur diffractometer using graphite-monochromated Mo K$\alpha$ radiation equipped with an Eos CCD detector ($\lambda$ = 0.71073 Å). MALDI-TOF mass spectra were measured on a Bruker UltrafleXtreme spectrometer and are calibrated against red phosphorus. Elemental analyses were conducted by Mr. Stephen Boyer at the London Metropolitan University. $H_4L^a$ and $H_4L^b$ were prepared according to published procedures, and 1 M $ZnEt_2$ in hexanes and $Zn\{N(SiMe_3)_2\}_2$ were used as supplied (Sigma-Aldrich). DFT calculations were conducted using the Gaussian09 package at the University of Edinburgh.

**Synthesis of 1a.** To a brown solution of $H_4L^a$ (0.41 g, 0.45 mmol) in THF (20 $cm^3$) was added a solution of $Zn\{N(SiMe_3)_2\}_2$ (0.36 $cm^3$, 0.90 mmol) in THF (ca. 2 $cm^3$) at room temperature. The mixture was stirred for 24 h, after which the solvent was removed under vacuum, yielding a brown solid that was dried under vacuum at 70 °C. Yield: 0.43 g (91%). $^1$H NMR ($C_6D_6$, 300 K): $\delta_H$/ppm 7.79 (s, 4H, imine), 6.99 (s, 2H, *meso*-H), 6.80 (d, 4H, $^3J_{HH}$ = 5 Hz, pyrrole $\beta$-H), 6.73 (s, 4H, Ar-H), 6.42 (d, 4H, $^3J_{HH}$ = 5 Hz, pyrrole $\beta$-H), 2.00 (s, 12H, Ar-$CH_3$). $^{13}C\{^1H\}$ NMR ($C_6D_6$, 300 K): $\delta_C$/ppm 150.47 (pyrrole $\alpha$-C, next to *meso*-position), 146.83 (imine), 146.40 (d, $^1J_{CF}$ = 246 Hz, $Ar^F$ *o*-C), 140.00 (pyrrole $\alpha$-C, next to imine), 137.9 (d, $^1J_{CF}$ = 242 Hz, overlapping $Ar^F$ *m*- and *p*-C), 136.79 (Ar, next to imine-N), 134.22 ($Ar^F$, next to *meso*-C), 133.76 (Ar, next to $CH_3$), 119.71 (pyrrole $\beta$-C), 116.30 (Ar C–H), 114.87 (pyrrole $\beta$-C), 42.15 (*meso*-C), 19.74 (Ar-$CH_3$). $^{19}F\{^1H\}$ NMR ($C_6D_6$, 300 K): $\delta_F$/ppm −139.9 (d, 4F, $^3J_{FF}$ = 20 Hz, $Ar^F$ *o*-F), −158.16 (t, 2F, $^3J_{FF}$ = 20 Hz, $Ar^F$ *p*-F), −163.75 (t, 4F, $^3J_{FF}$ = 20 Hz, $Ar^F$ *m*-F). MALDI-TOF-MS (DCTB): *m*/*z* 1063, $[C_{50}H_{30}F_{10}N_8Zn_2, M^+ + H]$. Anal. Calcd for $C_{50}H_{30}F_{10}N_8Zn_2$ ($M_r$ = 1063.6): C, 56.46; H, 2.84; N, 10.54. Found: C, 56.28; H, 2.95; N, 10.42.

**Synthesis of 1b.** This compound was prepared as described for **1a**. To a solution of $H_4L^b$ (0.50 g, 0.46 mmol) in THF (50 $cm^3$) was added $Zn\{N(SiMe_3)_2\}_2$ (0.391 g, 1.0 mmol). The crude product was washed with pentane (3 × 2 $cm^3$) and dried at 60 °C. Yield: 0.398 g (71.2%). Data for the major isomer are as follows. $^1$H NMR ($d_8$-THF, 300 K): $\delta_H$/ppm 8.66 (s, 2H, 9-anth), 8.21 (s, 4H, imine), 7.84 (s, 2H, 10-anth), 7.29 (d, 4H, $^3J_{HH}$ = 8.4 Hz, 2,7-anth), 6.84 (t, 4H, $^3J_{HH}$ = 10 Hz, 3,6-anth, overlap with minor isomer), 6.78 (d, 4H, $^3J_{HH}$ = 6.3 Hz, 4,5-anth), 6.43 (d, 4H, $^3J_{HH}$ = 3.4 Hz, pyrrole $\beta$-H), 5.72 (d, 4H, $^3J_{HH}$ = 3.4 Hz, pyrrole $\beta$-H), 5.69 (s, 2H, *meso*-H). Data for the minor isomer are as follows. $^1$H NMR ($d_8$-THF, 300 K): $\delta_H$/ppm 8.56 (s, 2H, 9-anth), 8.00 (s, 4H, imine), 7.77 (s, 2H, 10-anth), 7.24 (d, 4H, $^3J_{HH}$ = 8.6 Hz, 2,7-anth), 6.84 (t, 4H, $^3J_{HH}$ = 10 Hz, 3,6-anth), 6.70 (d, 4H, $^3J_{HH}$ = 6.7 Hz, 4,5-anth), 6.32 (d, 4H, $^3J_{HH}$ = 3.4 Hz, pyrrole $\beta$-H), 6.06 (d, 4H, $^3J_{HH}$ = 3.4 Hz, pyrrole $\beta$-H), 5.99 (s, 2H, *meso*-H). $^{13}C\{^1H\}$ NMR ($d_8$-THF, 300 K): $\delta_C$/ppm 158.56, 148.53, 146.2 (d, $^1J_{CF}$ = 249 Hz, $Ar^F$), 141.2 (d, $^1J_{CF}$ = 244 Hz, $Ar^F$), 138.6 (d, $^1J_{CF}$ = 260 Hz, $Ar^F$), 135.38, 134.09, 133.13, 129.08, 127.34, 127.18, 126.73, 124.83, 119.22, 117.67, 115.65, 112.58, 36.25. Data for the major isomer are as follows. $^{19}F\{^1H\}$ NMR ($d_8$-THF, 300 K): $\delta_F$/ppm −144.68 (d, 4F, $^3J_{FF}$ = 22.4 Hz, $Ar^F$ *o*-F, overlap with minor isomer), −160.25 (t, 2F, $^3J_{FF}$ = 21.8 Hz, $Ar^F$ *p*-F), −165.31 (t of d, 4F, $^3J_{FF}$ = 30.5 Hz, $Ar^F$ *m*-F). Data for the minor isomer are as follows. $^{19}F\{^1H\}$ NMR ($d_8$-THF, 300 K): $\delta_F$/ppm −144.68 (d, 4F, $^3J_{FF}$ = 22 Hz, $Ar^F$ *o*-F), −161.27 (t, 2F, $^3J_{FF}$ = 22 Hz, $Ar^F$ *p*-F), −165.76 (broad t, 4F, $Ar^F$ *m*-F). Anal. Calcd for $C_{62}H_{30}F_{10}N_8Zn_2$ ($M_r$ = 1207.76): C, 61.66; H, 2.50; N, 9.28. Found: C, 61.45; H, 2.35; N, 9.16.

**Synthesis of 2a.** A brown solution of $H_4L^a$ (0.10 g, 0.1 mmol) in THF (10 $cm^3$) was treated with a solution of $ZnEt_2$ in hexanes (0.5 $cm^3$, 1 mol $dm^{-3}$, 0.5 mmol) at −80 °C; the solution turned dark yellow. The mixture was warmed to room temperature and stirred for 18 h, after which the solvent was removed under vacuum, giving a dark yellow solid that was dried under vacuum at 70 °C. Yield: 0.12 g (94%). $^1$H NMR ($C_6D_6$, 300 K): $\delta_H$/ppm 7.68 (s, 4H, imine), 6.75 (d, 4H, $^3J_{HH}$ = 3.2 Hz, pyrrole $\beta$-H), 6.55 (s, 4H, Ar C–H), 6.26 (d, 4H, $^3J_{HH}$ = 1.9 Hz, pyrrole $\beta$-H), 6.03 (s, 2H, *meso*-H), 1.99 (s, 12H, Ar-$CH_3$), 1.32 (t, 12H, $^3J_{HH}$ = 8.1 Hz, ethyl-$CH_3$), 0.42 (q, 8H, $^3J_{HH}$ = 7.9 Hz, ethyl-$CH_2$). $^{13}C\{^1H\}$ NMR ($C_6D_6$, 300 K): $\delta_C$/ppm 156.71 (imine), 149.64 (pyrrole $\alpha$-C), 149.03 ($Ar^F$, next to *meso*-C), 145.9 (d, $^1J_{CF}$ = 248 Hz, $Ar^F$ *o*-C), 140.6 (d, $^1J_{CF}$ = 251 Hz, $Ar^F$ *p*-C), 139.44 (Ar, next to imine-N), 138.2 (d, $^1J_{CF}$ = 250 Hz, $Ar^F$ *m*-C), 137.79 (pyrrole $\alpha$-C), 134.78 (Ar, next to $CH_3$), 124.38 (Ar C–H), 122.04 (pyrrole $\beta$-C, nearest to imine), 114.27 (pyrrole $\beta$-C, nearest to *meso*-C), 40.10 (*meso*-C), 19.20 (Ar-$CH_3$), 12.59 (ethyl-$CH_3$), 0.07 (ethyl-$CH_2$). $^{19}F\{^1H\}$ NMR ($C_6D_6$, 333 K): $\delta_F$/ppm −140.24 (broad s, 3F, $Ar^F$ *o*-F), −156.94 (t, 2F, $^3J_{FF}$ = 21.9 Hz, $Ar^F$ *p*-F), −162.26 (t of d, $^3J_{FF}$ = 23.0, 8.1 Hz, $Ar^F$ *m*-F). Anal. Calcd for $C_{58}H_{50}F_{10}N_8Zn_4$ ($M_r$ = 1310.7): C, 53.15; H, 3.85; N, 8.55. Found: C, 52.87; H, 3.71; N, 8.46.

**Synthesis of 2b.** This compound was prepared as described for **2a**. To a solution of $H_4L^b$ (0.20 g, 0.18 mmol) in THF (30 $cm^3$) was added a solution of $ZnEt_2$ in hexanes (0.75 cm3, 1 mol $dm^{-3}$, 0.75 mmol). Yield: 0.128 g (49%). $^1$H NMR ($d_8$-THF, 300 K): $\delta_H$/ppm 8.89 (s, 2H, 9-anth), 8.55 (s, 2H, 10-anth), 8.40 (s, 4H, imine), 7.84 (d, 4H, $^3J_{HH}$ = 7.0 Hz, 2,7-anth), 7.44 (dd, 4H, $^3J_{HH}$ = 5.0 Hz, 3,6-anth), 7.14 (d, 4H, $^3J_{HH}$ = 5.1 Hz, 4,5-anth), 6.75 (s, 4H, pyrrole $\beta$-H), 6.54 (s, 4H, pyrrole $\beta$-H), 5.81 (s, 2H, *meso*-H), 0.99 (t, 12H, $^3J_{HH}$ = 7.5 Hz, ethyl-$CH_3$), 0.10 (q, 8H, $^3J_{HH}$ = 7.5 Hz, ethyl-$CH_2$). $^{13}C\{^1H\}$ NMR ($d_8$-THF, 300 K): $\delta_C$/ppm 158.43 (imine), 148.37 (1,8-anth), 146.87 (anth, quaternary-C), 145.3 (d, $^1J_{CF}$ = 246 Hz, $Ar^F$), 139.7 (d, $^1J_{CF}$ = 256 Hz, $Ar^F$), 137.6 (d, $^1J_{CF}$ = 255 Hz, $Ar^F$), 136.80 (pyrrole $\alpha$-C), 133.12 (pyrrole $\alpha$-C), 128.05 (10-anth), 127.21 ($Ar^F$, next to *meso*-C), 126.27 (3,6-anth), 125.44 (2,7-anth), 124.64 (anth, quaternary-C), 120.75 (pyrrole $\beta$-C), 118.17 (9-anth), 117.20 (4,5-anth), 114.02 (pyrrole $\beta$-C), 40.97 (*meso*-C), 12.11 (ethyl-$CH_3$), −3.21 (ethyl-$CH_2$). $^{19}F\{^1H\}$ NMR ($d_8$-THF, 333 K): $\delta_F$/ppm −140.27 (broad s, 2F, $Ar^F$ *o*-F), −161.21 (t, 2F, $^3J_{FF}$ = 20 Hz, $Ar^F$ *p*-F), −164.93 (broad t, 4F, $^3J_{FF}$ = 18 Hz, $Ar^F$ *m*-F). Anal. Calcd for $C_{70}H_{50}F_{10}N_8Zn_4$ ($M_r$ = 1454.82): C, 57.79; H, 3.46; N, 7.70. Found: C, 57.68; H, 3.52; N, 7.62.

**Synthesis of 3.** **2a** (10 mg, 8 $\mu$mol) was dissolved in a solution of $H_2O$ in $C_6D_6$ (concentration of $H_2O$ 8.6 mM by $^1$H NMR integration, 0.9 $cm^3$, 8 $\mu$mol of $H_2O$). Yield: 5 mg (50% conversion by $^1$H NMR integration). $^1$H NMR ($C_6D_6$): $\delta_H$/ppm 7.95 (s, 4H, imine), 6.90 (d, 4H, $^3J_{HH}$ = 5 Hz, pyrrole $\beta$-H), 6.58 (s, 4H, Ar C–H), 6.43 (s, 2H, *meso*-H), 6.22 (broad s, 4H, pyrrole $\beta$-H), 2.05 (s, 12H, Ar-$CH_3$), 1.51 (t, 6H, $^3J_{HH}$ = 10 Hz, ethyl-$CH_3$), 0.30 (q, 4H, $^3J_{HH}$ = 10 Hz, ethyl-$CH_2$). $^{13}C\{^1H\}$ NMR ($d_8$-THF, 300 K): $\delta_C$/ppm 153.59 (imine), 148.90 ($Ar^F$, next to *meso*-C), 147.1 (d, $^1J_{CF}$ = 246 Hz, $Ar^F$), 142.56


DOI: 10.1021/om501244n
Organometallics XXXX, XXX, XXX–XXX

(Ar, next to imine), 139.11 (d, $^1J_{CF}$ = 251 Hz, $Ar^F$), 138.74 (Ar, next to $CH_3$), 135.4 (pyrrole $\alpha$-C, next to *meso*-C), 124.09 (pyrrole $\alpha$-C, next to imine), 121.65 (Ar C–H), 119.72 (pyrrole $\beta$-C), 118.21 (d, $^1J_{CF}$ = 246 Hz, $Ar^F$), 112.00 (pyrrole $\beta$-C), 32.69 (*meso*-C), 19.57 ($CH_3$, Ar), 7.13 (ethyl-$CH_3$), 2.53 (ethyl-$CH_2$). $^{19}F\{^1H\}$ NMR ($d_8$-THF, 300 K): $\delta_F$/ppm −137.74 (d, 4F, $^3J_{FF}$ = 20 Hz, $Ar^F$ *o*-F), −158.72 (t, 2F, $^3J_{FF}$ = 20 Hz, $Ar^F$ *p*-F), −164.52 (t of d, 4F, $^3J_{FF}$ = 25, 5 Hz, $Ar^F$ *m*-F).

**Synthesis of 4.** To a solution of **2b** (0.180 g, 0.167 mmol) in THF (10 $cm^3$) was added $H_2O$ previously degassed with $N_2$ (12 $\mu$L, 0.67 mmol). The solution was stirred for 1 h, after which the solvent was removed under vacuum, yielding a red solid that was dried under vacuum at 60 °C. Yield: 0.209 g (82%). $^1H$ NMR ($d_8$-THF, 300 K): $\delta_H$/ppm 9.78 (s, 2H, 9-anth), 8.45 (s, 4H, imine), 8.43 (s, 2H, 10-anth), 7.76 (d, 4H, $^3J_{HH}$ = 10 Hz, 2,7-anth), 7.35 (t, 4H, $^3J_{HH}$ = 10 Hz, 3,6-anth), 7.12 (d, 4H, $^3J_{HH}$ = 10 Hz, 4,5-anth), 6.86 (d, 4H, $^3J_{HH}$ = 3.4 Hz, pyrrole $\beta$-H), 6.54 (d, 4H $^3J_{HH}$ = 3.4 Hz, pyrrole $\beta$-H), 6.44 (s, 2H, *meso*-H), 4.14 (s, 2H, $\mu^2$-OH), 3.36 (s, 2H, $\mu^2$-OH). $^{13}C\{^1H\}$ NMR ($d_8$-THF, 300 K): $\delta_C$/ppm 156.67, 149.81, 148.32, 138.28, 133.74, 129.00, 128.95, 126.66, 126.43, 122.93, 117.63, 117.06, 113.21, 42.64. Anal. Calcd for $C_{62}H_{34}F_{10}N_8O_4Zn_4$ ($M_r$ = 1406.61): C, 52.95; H, 2.44; N, 7.97. Found: C, 50.04; H, 1.83; N, 6.77.

## ■ ASSOCIATED CONTENT

### Supporting Information

Figures, tables, and CIF files giving variable-temperature $^1H$ and $^{19}F$ NMR data, MALDI-MS data, computational details and results, and X-ray crystallographic data. This material is available free of charge via the Internet at http://pubs.acs.org.

## ■ AUTHOR INFORMATION


### Corresponding Author

*E-mail for J.B.L.: jason.love@ed.ac.uk.


### Notes

The authors declare no competing financial interest.

## ■ ACKNOWLEDGMENTS

We thank the University of Edinburgh, the EPSRC (EP/J010890/1), and the EPSRC CRITICAT Centre for Doctoral Training (Ph.D. studentship to M.C.; Grant code EP/L016419/1) for financial support.

## ■ DEDICATION

This article is dedicated to the memory of Professor Michael F. Lappert FRS.

## ■ REFERENCES


(1) Dempsey, J. L.; Esswein, A. J.; Manke, D. R.; Rosenthal, J.; Soper, J. D.; Nocera, D. G. *Inorg. Chem.* **2005**, *44*, 6879–6892.
(2) Holm, R. H.; Kennepohl, P.; Solomon, E. I. *Chem. Rev.* **1996**, *96*, 2563.
(3) Dance, I. *Chem. Commun.* **2013**, *49*, 10893–10907.
(4) Kaila, V. R. I.; Verkhovsky, M. I.; Wikström, M. *Chem. Rev.* **2010**, *110*, 7062–7081.
(5) Friedle, S.; Reisner, E.; Lippard, S. J. *Chem. Soc. Rev.* **2010**, *39*, 2768–2779.
(6) Dau, H.; Limberg, C.; Reier, T.; Risch, M.; Roggan, S.; Strasser, P. *ChemCatChem* **2010**, *2*, 724–761.
(7) Gloaguen, F.; Rauchfuss, T. B. *Chem. Soc. Rev.* **2009**, *38*, 100–108.
(8) Horak, K. T.; Velian, A.; Day, M. W.; Agapie, T. *Chem. Commun.* **2014**, *50*, 4427–4429.
(9) Dalle, K. E.; Gruene, T.; Dechert, S.; Demeshko, S.; Meyer, F. *J. Am. Chem. Soc.* **2014**, *136*, 7428–7434.
(10) Kanady, J. S.; Lin, P.-H.; Carsch, K. M.; Nielsen, R. J.; Takase, M. K.; Goddard, W. A.; Agapie, T. *J. Am. Chem. Soc.* **2014**, *136*, 14373–14376.
(11) Lionetti, D.; Day, M. W.; Agapie, T. *Chem. Sci.* **2013**, *4*, 785–790.
(12) Tereniak, S. J.; Carlson, R. K.; Clouston, L. J.; Young, V. G.; Bill, E.; Maurice, R.; Chen, Y.-S.; Kim, H. J.; Gagliardi, L.; Lu, C. C. *J. Am. Chem. Soc.* **2013**, *136*, 1842–1855.
(13) Tsui, E. Y.; Kanady, J. S.; Day, M. W.; Agapie, T. *Chem. Commun.* **2011**, *47*, 4189–4191.
(14) Cao, R.; Müller, P.; Lippard, S. J. *J. Am. Chem. Soc.* **2010**, *132*, 17366–17369.
(15) Gavrilova, A. L.; Bosnich, B. *Chem. Rev.* **2004**, *104*, 349.
(16) Pace, R. J.; Stranger, R.; Petrie, S. *Dalton Trans.* **2012**, *41*, 7179–7189.
(17) Kanady, J. S.; Tsui, E. Y.; Day, M. W.; Agapie, T. *Science* **2011**, *333*, 733–736.
(18) Powers, T. M.; Betley, T. A. *J. Am. Chem. Soc.* **2013**, *135*, 12289–12296.
(19) Powers, T. M.; Fout, A. R.; Zheng, S.-L.; Betley, T. A. *J. Am. Chem. Soc.* **2011**, *133*, 3336–3338.
(20) Murray, L. J.; Weare, W. W.; Shearer, J.; Mitchell, A. D.; Abboud, K. A. *J. Am. Chem. Soc.* **2014**, *136*, 13502–13505.
(21) Love, J. B. *Chem. Commun.* **2009**, 3154–3165.
(22) Devoille, A. M. J.; Love, J. B. *Dalton Trans.* **2012**, *41*, 65–72.
(23) Givaja, G.; Volpe, M.; Edwards, M. A.; Blake, A. J.; Wilson, C.; Schroder, M.; Love, J. B. *Angew. Chem., Int. Ed.* **2007**, *46*, 584–586.
(24) Askarizadeh, E.; Devoille, A. M. J.; Boghaei, D. M.; Slawin, A. M. Z.; Love, J. B. *Inorg. Chem.* **2009**, *48*, 7491–7500.
(25) Arnold, P. L.; Jones, G. M.; Odoh, S. O.; Schreckenbach, G.; Magnani, N.; Love, J. B. *Nat. Chem.* **2012**, *4*, 221–227.
(26) Arnold, P. L.; Patel, D.; Wilson, C.; Love, J. B. *Nature* **2008**, *451*, 315–317.
(27) Arnold, P. L.; Pecharman, A.-F.; Hollis, E.; Yahia, A.; Maron, L.; Parsons, S.; Love, J. B. *Nat. Chem.* **2010**, *2*, 1056–1061.
(28) Givaja, G.; Blake, A. J.; Wilson, C.; Schroder, M.; Love, J. B. *Chem. Commun.* **2005**, 4423–4425.
(29) Leeland, J. W.; White, F. J.; Love, J. B. *J. Am. Chem. Soc.* **2011**, *133*, 7320–7323.
(30) Pankhurst, J. R.; Cadenbach, T.; Betz, D.; Finn, C.; Love, J. B. *Dalton Trans.* **2014**, *44*, 2066–2070.
(31) Tomat, E.; Cuesta, L.; Lynch, V. M.; Sessler, J. L. *Inorg. Chem.* **2007**, *46*, 6224–6226.
(32) Devoille, A. M. J.; Richardson, P.; Bill, N. L.; Sessler, J. L.; Love, J. B. *Inorg. Chem.* **2011**, *50*, 3116–3126.
(33) Redshaw, C.; Elsegood, M. R. J. *Angew. Chem., Int. Ed.* **2007**, *46*, 7453–7457.
(34) Allen, F. *Acta Crystallogr., Sect. B* **2002**, *58*, 380–388.
(35) Lesikar, L. A.; Richards, A. F. *Polyhedron* **2010**, *29*, 1411–1422.
(36) Pettersen, A.; Lennartson, A.; Håkansson, M. *Organometallics* **2009**, *28*, 3567–3569.
(37) Bury, W.; Krajewska, E.; Dutkiewicz, M.; Sokolowski, K.; Justyniak, I.; Kaszkur, Z.; Kurzydlowski, K. J.; Plocinski, T.; Lewinski, J. *Chem. Commun.* **2011**, *47*, 5467–5469.
(38) Agnew, C.; Dillon, K. B.; Goeta, A. E.; Thompson, A. L. *Inorg. Chim. Acta* **2009**, *362*, 4260–4262.
(39) Sokolowski, K.; Bury, W.; Justyniak, I.; Cieslak, A. M.; Wolska, M.; Soltys, K.; Dziecielewski, I.; Lewinski, J. *Chem. Commun.* **2013**, *49*, 5271–5273.
(40) Buchard, A.; Jutz, F.; Kember, M. R.; White, A. J. P.; Rzepa, H. S.; Williams, C. K. *Macromolecules* **2012**, *45*, 6781–6795.
(41) Kember, M. R.; Buchard, A.; Williams, C. K. *Chem. Commun.* **2011**, *47*, 141–163.
(42) MacDowell, N.; Florin, N.; Buchard, A.; Hallett, J.; Galindo, A.; Jackson, G.; Adjiman, C. S.; Williams, C. K.; Shah, N.; Fennell, P. *Energy Environ. Sci.* **2010**, *3*, 1645–1669.




DOI: 10.1021/om501244n
*Organometallics* XXXX, XXX, XXX–XXX